

# Flow and heat transfer in a closed loop thermosyphon. Part I – theoretical simulation

---

R T Dobson

J C Ruppertsberg

*Department of Mechanical Engineering, University of Stellenbosch*

## **Abstract**

*A natural circulation, closed loop thermosyphon can transfer heat over relatively large distances without any moving parts such as pumps and active controls. Such loops are thus considered suitable for nuclear reactor cooling applications where safety and high reliability are of paramount importance. A theoretical basis from which to predict the flow and heat transfer performance of such a loop is presented. A literature survey of the background theory is undertaken and the theoretical equations describing the single and two-phase flow as well as heat transfer behaviour are given. The major assumptions made in deriving these equations are that the working fluid flow is quasi-static and that its single, two-phase flow and heat transfer behaviour may be captured by dividing the working fluid in the loop into a number of one dimensional control volumes and then applying the equations of change to each of these control volumes. Theoretical simulations are conducted for single phase, single and two-phase and heat pipe operating modes, and a sensitivity analysis of the various variables is undertaken. It is seen that the theoretical results capture the single and two-phase flow operating modes well for a loop that includes an expansion tank, but not for the heat pipe operating mode. It is concluded that the theoretical model may be used to study transient and dynamic non-linear effects for single and two-phase modes of operation. To more accurately predict the heat transfer rate of the loop however, loop specific heat transfer coefficients need to be determined experimentally and incorporated into the theoretical model.*

*Keywords: closed loop two-phase thermosyphon, natural circulation loop, two-phase flow, theoretical modelling, transient analysis*

## **1. Introduction**

A closed loop thermosyphon is an energy-transfer device capable of transferring heat from a heat source to a separate heat sink over a relatively long distance, without the use of active control instrumentation and any mechanically moving parts such as pumps. These devices are thus particularly suitable for cooling applications (as in nuclear reactor technology, for example) where reliability and safety are of paramount importance.

The closed loop thermosyphon may be visualised as a long hollow pipe, bent and the ends joined to form a continuous loop, filled with working fluid and orientated in a vertical plane. If the one side of the loop is heated and the other side cooled, the average density of the fluid in the heated side is less than in the cooled side. An essentially hydrostatic pressure difference, as a result of the thermally induced temperature gradient between the hot and the cold sides, drives the fluid flows around the loop. The ‘buoyancy’ force, as it is often termed, driving the fluid is in turn counteracted by an opposing frictional force that tends to retard the flow.

The use of such a natural circulation closed loop thermosyphon is being considered for the cooling of the reactor cavity of a Pebble Bed Modular Reactor (PBMR). Loop thermosyphons exhibit complex transient flow behaviour during start-up, shut-down and other sudden changes in loop operating conditions. Capturing this complex behaviour analytically using a theoretically sound platform is required to supplement the experimental verification of the loop’s ability to perform its heat transfer duty reliably under all normal operating and postulated accident conditions.

In this paper, a theoretical basis on which to analyse and predict the flow and heat transfer per-

formance of such a closed loop thermosyphon is presented. In particular, the rather complex transient and dynamic nature of the flow will be addressed. A limited literature study, giving a number of representative references supporting the theoretical modelling is undertaken. A number of simulated operating conditions are given, and finally, a discussion of the findings is given and conclusions drawn.

## 2. Background theory and literature survey

A relatively large amount of published literature is available relating to loop thermosyphons. To limit this section, only previous work undertaken to theoretically model the thermal hydraulic behaviour of the working fluid in the loop will be considered. Literature relating to purely experimental observations and demonstrations are considered in Part II of this paper.

Welander (1966) considered the fluid to be driven by the pressure difference and a buoyancy force, and is retarded by a frictional force. The assumptions made included:

- The Boussinesq approximation
- The tangential friction force on the fluid is proportional to the *instantaneous* flow rate
- The temperature of the fluid is uniform over each cross-sectional area
- The heat transfer rate between the pipe and the fluid is proportional to the difference between a prescribed wall temperature and the fluid

Applying these assumptions, the essentially *one-dimensional* equations of change are obtained for a single phase fluid. Using analytical as well as numerical integration, a stability map was constructed in which stable and unstable operating conditions were plotted and the occurrence of transient and non-linear effects established. The reason why this article has been singled out is that it is one of the earliest publications giving the assumptions on which most of the theoretical work to date has been based.

Grief (1988) gives a descriptive review of a number of single phase and two-phase thermosyphon loops but Knaai and Zvirin (1990, 1993) show how the single phase loop theory may be extended for the case of a two-phase loop by specifying suitable equations for the friction factor, the two-phase frictional multiplier, the single and two-phase heat transfer coefficients and a suitable relationship for the void and mass fractions. They solved their differential equations using a relatively involved combination of analytical and numerical stages. Dobson (1993), although only for a single phase laminar fluid, shows how a simple explicit finite difference discretisation formulation scheme is able to capture transients and the highly non-linear behaviour of the loop. Vincent and Kok (1992),

using only ten differential equations, were able to capture the transient performance of a two-phase closed loop thermosyphon. They also emphasize the value of the control volume approach as being a powerful tool to describe the overall performance of the thermosyphon with a limited number of variables.

Yun et al. (2005) applied the theory, as outlined in the preceding two paragraphs, to an instability analysis in the natural circulation loops of the China Advanced Research Reactor (CARR). They used 54 control volumes to represent the loop and a Gear multi-value method to solve the total set of 72 equations. They compared the calculated results with experimental data and concluded that the theoretical model is capable of simulating the non-linear dynamics of the CARR loop. Lee and Pan (2005) modelled an advanced boiling water reactor natural circulation loop earmarked for construction in Taiwan. They give a number of stability maps, undertook a number of parametric studies and identified periodic as well as chaotic oscillations. Lee and Kim (1999) investigated the role of an expansion tank fitted to a two-phase natural circulation loop.

Lee and Rhi (2000) considered methods for computer simulation of two-phase loop thermosyphons. They compared the computer simulations with 5 different experimental loops' maximum heat transfer rates ranging from 60 to 100 000 W. It was concluded that computer simulation alone could not give any meaningful results unless they are accompanied with empirical correlations using loop-specific experimental test results.

## 3. Closed loop thermosyphon theory

Three loop operating modes have been considered. The first is a single phase loop in which the pressure of the working fluid never exceeds the saturated vapour pressure associated with its temperature. In this case, the loop is provided with an expansion tank into which the excess fluid, as a result of thermal expansion, can flow. This prevents unnecessary high pressures. The second is a two-phase loop in which the working fluid is allowed to boil and condense. In this mode, the loop is also provided with an expansion tank to control the pressure in the loop. Thirdly, the loop is partially filled with liquid-phase working fluid but is not provided with an expansion tank. In this case, the working fluid not only boils and condenses, but also a significant amount of splashing and *geysering* occurs; this will be called for convenience, the *heat pipe* operating mode.

The physical layout of the loop to be theoretically modelled in this paper is shown in Figure 1, whilst the important dimensional parameters are given in Figure 2. This is an experimental loop (Dobson and Ruppertsberg, 2007) that has been

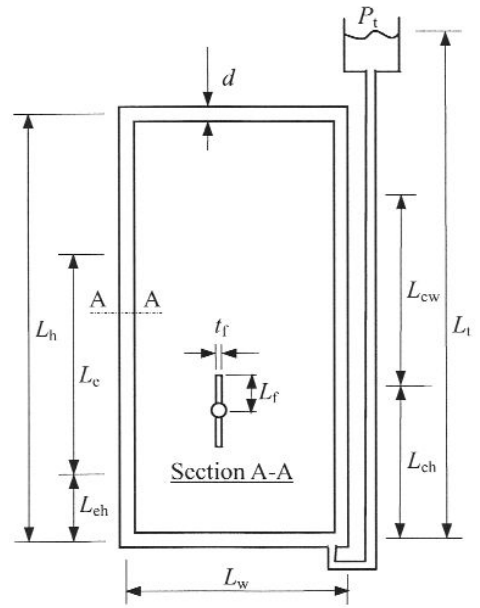
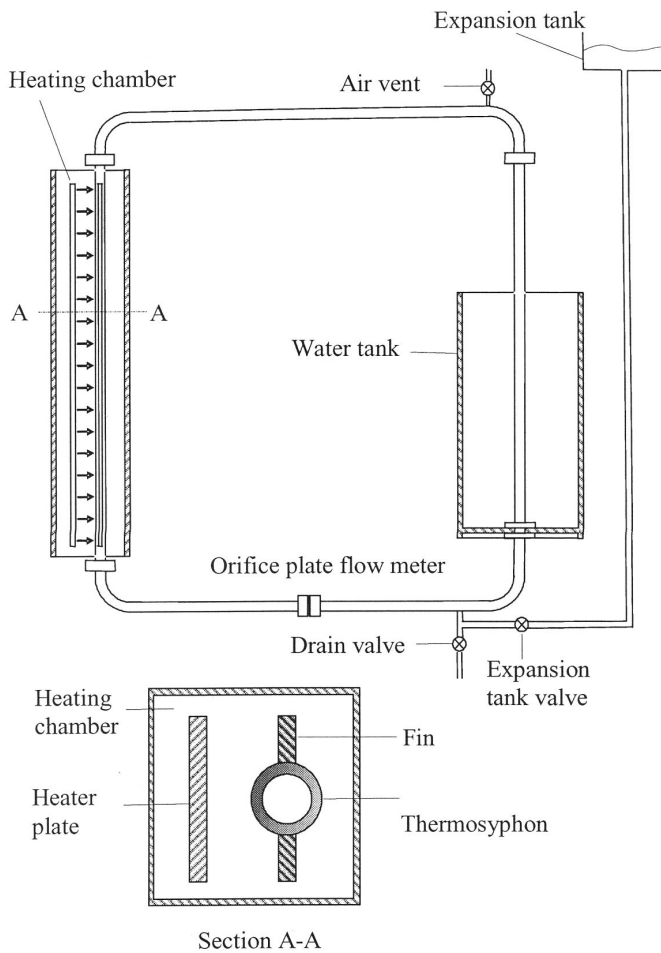


**Figure 2: Basic dimensions of the loop closed loop thermosyphon**

**Figure 1 (left): Schematic representation of a closed loop thermosyphon to be used in a reactor cavity cooling system**

constructed to represent a small-scale version of a possible full-size loop that is capable of cooling the concrete containment structure surrounding a nuclear reactor (Dobson, 2006). The heater plate heats the fins attached to the heated portion of the loop by radiation and convection. The heat is then transferred by conduction through the fins, to the inside surface of the pipe and by convection to the working fluid. In the cooled portion of the loop, heat is transferred from the working fluid to the water in the tank. The lower density of the fluid in the heated portion and the higher density in the cooled portion results in a pressure difference between the two legs of the loop. This results in fluid flows around the loop, upwards in the hot leg and downwards in the cooled leg.

To theoretically model the heat transferred, the loop is divided into a number of cylindrical control volumes. The equations of change are then applied: continuity, motion and energy; with appropriate state equations for closure. The most important assumptions made being one dimensional control volumes and quasi-static motion. The quasi-static assumption is motivated by the fact that the average velocity of the working fluid in the loop is two to three orders of magnitude less than the speed of sound in the fluid. This means that the rate at which pressure waves are propagated through the working fluid are

much faster than the rate at which mass and heat moves in the loop; hence it is safe to assume a quasi-static solution for the equation of motion.

Given a heating plate temperature-time profile, heat is transferred from the heating plate to the fins according to:

$$\dot{Q}_{p,f} = (T_p - T_f) / R_{p,f} \quad (1)$$

where  $R_{p,f} = R_{r,p,f} + R_{c,p,f}$ ,

$$R_{r,p,f} = \frac{1 - \epsilon_p + \frac{1}{F_{p,f} A_p} + \frac{1 - \epsilon_f}{A_f \epsilon_f}}{\sigma \left( (273 + T_p)^2 + (273 + T_f)^2 \right) \left( (273 + T_p) + (273 + T_f) \right)}$$

$$R_{c,p,f} = \frac{1}{h_{p,f} A_p} \quad \text{and} \quad A_p = A_f = L_f L$$

and where  $L$  is the length of the control volume.

The temperature of the fin is given by:

$$\frac{dT_f}{dt} = (\dot{Q}_{p,f} - \dot{Q}_{f,hp}) / (m_f c_{v,f}) \quad (2)$$

where  $\dot{Q}_{f,hp} = \frac{T_f - T_{hp}}{R_{f,hp}}$ ,  $m_f = \rho_f L_f t_f L$  and

$$R_{f,hp} = \frac{L_f/2}{k_f t_f L} + \frac{\ln(r_{o,hp}/r_{i,hp})}{2\pi k_{hp} L} + \frac{1}{2\pi r_{i,hp} L h_{i,hp}}$$

The internal energy of the fluid in the heat pipe for each control volume in the heated section of the loop is given by:

$$\frac{du}{dt} = (2\dot{Q}_{f, hp} + \dot{m}i_{in} - \dot{m}i_{out}) / (mc) \quad (3)$$

where  $m = \pi r_{i, hp}^2 L_i \rho$ .

The temperature and mass fraction are then determined, depending on whether the fluid is boiling (or condensing) by:

$$\text{If } u^{t+\Delta t} < u_i \text{ then } T_{hp}^{t+\Delta t} = u^{t+\Delta t} / c_v$$

$$\text{and } x^{t+\Delta t} = 0$$

$$\text{If } u^{t+\Delta t} > u_i \text{ then } T_{hp}^{t+\Delta t} = T_{sat}$$

$$\text{and } x^{t+\Delta t} = u^{t+\Delta t} - u_f^{t+\Delta t} / u_{fg}^{t+\Delta t}$$

where  $u_{hp} = u_f + xu_{fg}$ ,  $i = i_f + xi_{fg}$ ,

$$u_f = c_v T_{hp} \text{ and } i_f = c_p T_{hp}.$$

The internal energy of the fluid in the heat pipe for each control volume of the cooled section of the loop is given by:

$$\frac{du}{dt} = (\dot{Q}_{hp, cw} + \dot{m}i_{in} - \dot{m}i_{out}) / (mc) \quad (4)$$

In the cooled portion of the loop the temperature, mass fraction of fluid and properties are determined using the same identities as applicable for boiling except that now condensation takes place and the heat transfer rate will depend on the rate at which heat is transferred to the heat sink cooling water – i.e.:

$$\dot{Q}_{hp, cw} = \frac{T_{hp} - T_{cw}}{R_{hp, cw}}, \text{ and}$$

$$R_{hp, cw} = \frac{1}{2\pi r_{i, hp} h_{i, hp}} + \frac{\ln(r_{o, hp} / r_{i, hp})}{2\pi k_{hp} L} + \frac{1}{2\pi r_{o, hp} h_{o, hp}}$$

The mass flow rate of the fluid circulating in the heat pipe is determined by conducting a momentum balance around the loop and is given by (Dobson, 2006):

$$\frac{d\dot{m}}{dt} = \frac{\sum_{k=1}^{N_k} \rho_k L_k g \sin \phi_k}{\sum_{k=1}^{N_k} \frac{L_k}{A_{x, k}}} - \frac{\sum_{k=1}^{N_k} \frac{C_{f, \ell o, k} \phi_{\ell o, k}^2 L_k + L_{f, equiv, k}}{\rho_k r_{i, hp} A_{x, k}^2} \dot{m}^2}{\sum_{k=1}^{N_k} \frac{L_k}{A_{x, k}}} \quad (5)$$

In equation (5)  $\phi_k$  is the angle between the flow direction and the horizontal and  $\phi_{\ell o, k}^2$  is the two-phase liquid only frictional multiplier (Whalley, 1990). The first term on the right hand is the buoyancy term tending to force the fluid around the loop, while the last term is the friction term tending to retard the flow.  $L_k$  is the length of the  $k$ 'th of  $N_k$  control volume and  $L_{f, equiv, k}$  is the equivalent length of pipe taking the minor losses associated with the  $k$ 'th control volume into account (for example, entrance, exit, contraction, expansion and bend losses).

Suitable closure relationships, equations and/or correlations are required for the working fluid properties, for example, the density  $\rho$ , viscosity  $\mu$ , thermal conductivity  $k$ , specific heat  $c$ , and the coefficient of friction  $C_f$ , heat transfer coefficients  $h$ , and void fraction  $\alpha$ . Many existing closure correlations are available but as explained by Lee and Rhi (2000), it is doubtful whether they are accurate enough unless they are experimentally verified using the same physical loop that is being theoretically modelled. Indeed they suggest that a simple *lumped* method, that does not necessarily distinguish between the different flow patterns that are commonly used to describe two-phase flow regimes, can be used.

The above theory applies to the single and single and two-phase operating modes. To theoretically simulate the heat pipe mode of operation is more problematic due to the considerably more complex behaviour of the working fluid in the loop. The simultaneous occurrence of special two-phase phenomenon such as geysering, splashing and counter current flow, as yet, defies a rigid mathematical and theoretical basis. To overcome this problem the entire loop is considered as a single control volume. With these approximating assumptions the heat transfer rate from the average fin at temperature,  $T_f$ , to the working fluid at temperature,  $T_{hp}$ , in the loop must equal the heat transfer rate from the cooled portion of the loop to the cooling water:

$$\dot{Q}_{f, hp} = \frac{T_f - T_{hp}}{R_{f, hp}} = \dot{Q}_{hp, cw} = \frac{T_{hp} - T_{cw}}{R_{hp, cw}} \quad (6)$$

On rearranging equation (6) the working fluid temperature is given by

$$T_{hp} = \frac{T_f R_{hp, cw} + T_{cw} R_{f, hp}}{R_{hp, cw} + R_{f, hp}}, \quad (7)$$

where the thermal resistances have already been defined in equations (2) and (4).

#### 4. Theoretical simulation

The system of differential equations defining the behaviour of the loop as given in the previous sec-

tion is conveniently solved using a fully explicit numerical formulation. Table 1 gives the basic dimensions and parameters for a typical loop, termed the *base-case*.

**Table 1: Base-case loop dimensions and parameters (see Figure 2 and nomenclature)**

|   |
|---|
| $d = 22.4 \text{ mm}$ , $L_h = 1.7 \text{ m}$ , $L_w = 1.6 \text{ m}$   |
| $L_f = 72.3 \text{ mm}$ , $t_f = 3 \text{ mm}$  |
| $L_{eh} = 100 \text{ mm}$ , $L_e = 1.5 \text{ m}$ , $L_{ch} = 100 \text{ mm}$ ,<br>$L_{cw} = 1.5 \text{ m}$   |
| $P_t = 100 \text{ kPa}$ , $L_t = 2.00 \text{ m}$  |
| $\varepsilon_p = 0.3$ , $\varepsilon_f = 0.3$   |
| $h_{eo} = 5 \text{ W/m}^2\text{K}$ , $h_{ei} = 1\,200 \text{ W/m}^2\text{K}$ ,<br>$h_{co} = 1\,200 \text{ W/m}^2\text{K}$ , $h_{ci} = 1\,200 \text{ W/m}^2\text{K}$ |
| working fluid = water   |
| $h_{hp,e,i} = 3\,000 \text{ W/m}^2\text{K}$ , $h_{hp,c,i} = 2\,200 \text{ W/m}^2\text{K}$   |

The following closure equations were used. For a single phase control volume:

$$C_{f,k} = 1 \text{ if } \text{Re}_{\ell_0,k} \leq 1,$$

$$C_{f,k} = 16/\text{Re}_{\ell_0,k} \text{ if } 1 < \text{Re}_{\ell_0,k} \leq 1181$$

$$C_{f,k} = 0.079 \text{Re}_{\ell_0,k}^{-0.25} \text{ if } \text{Re}_{\ell_0,k} > 1181$$

where  $\text{Re}_{\ell_0} = \frac{4\dot{m}}{\pi 2r_{i,hp}\mu_\ell}$ .

For two-phase flow, the coefficient of friction of a two-phase control volume is assumed as the single phase coefficient of friction multiplied by the so-called two-phase flow frictional multiplier:

$$C_{f,k} = C_{f,\ell_0,k} \phi_{\ell_0,k}^2$$

The two-phase frictional multiplier may be given, assuming turbulent flow for both the phases, in terms of the so called Martinelli parameter (Carey, 1992) as:

$$\phi_{\ell_0,k}^2 = \phi_{tt}^2 (1-x)^{1.75}$$

Where  $\phi_{tt}^2 = 1 + 20/X_{tt} + 1/X_{tt}^2$ ,

and  $X_{tt} = \left(\frac{\rho_g}{\rho_\ell}\right)^{0.5} \left(\frac{\mu_\ell}{\mu_g}\right)^{0.125} \left(\frac{1-x}{x}\right)^{0.875}$

For two-phase flow the void fraction may be given by the Lockhart-Martinelli correlation (Carey, 1992):

$$\alpha = \left(1 + 0.28 X_{tt}^{0.71}\right)^{-1}, \text{ the density by}$$

$$\rho = \alpha \rho_v + (1-\alpha) \rho_\ell \text{ and the two-phase properties}$$

may be approximated as

$$\mu = \left[\frac{x}{\mu_v} + \frac{(1-x)}{\mu_\ell}\right]^{-1}, \quad c = x c_v + (1-x) c_\ell \text{ and}$$

$$k = \alpha k_v + (1-\alpha) k_\ell.$$

Any suitable correlations may be used for the single phase vapour and liquid properties. Numerous and invariable complicated correlations are available for the single and the two-phase heat transfer coefficients. Rather than complicate the theoretical model further by making use of these correlations (which are not necessarily applicable for this geometry and operating conditions), constant heat transfer coefficients have been used of values as reflected in Table 1.

The mass flow rate, working fluid temperatures and heat transfer rates for a given plate temperature of a theoretical simulation, using the initial conditions and values reflected in Table 1, are shown in Figures 3 to 5. The given plate temperature  $T_p$  as a function of time is seen in Figure 3 to increase from 20 to 400°C in 1000 s remaining steady for 2000 s and then decrease in a further 2000 s back to 20°C.

In response to the plate temperature, the mass flow rate of the working fluid in the closed loop thermosyphon is seen in Figure 3 to increase to 18 g/s, drop down to 14 g/s in about 100 s and then increase again steadily to about 32 g/s as the plate reached its maximum temperature. The mass flow rate then remains steady and before decreasing as the plate temperature decreases. The temperatures of the fin  $T_f$  and the working fluid  $T_{hp}$  respond to the plate temperature as shown in Figure 4. The temperature of the fin at the top of the loop is its hottest, at about 125°C, and some at the bottom of the loop about 20°C less. The temperature of the working fluid follows the fin temperature but at some 30°C less. The heat input in the evaporator section  $\dot{Q}_e$  and removed in the condenser  $\dot{Q}_c$  is shown in Figure 4. Both curves are similar but as expected the heat removed lags the heat input by about 200 s.

In the simulation shown in Figures 3 to 5, boiling did not occur. To further investigate the behaviour of the loop, a sensitivity analysis was conducted by determining the response of the theoretical prediction while changing only one variable at a time; the results of this analysis are given in Table 2. It is seen that varying the static pressure had an insignificant effect on the heat transfer performance of the loop. Heating only the lower half and cooling only the top half (No. 3) increased the mass flow rate, but reduced the heat transfer rate. Exposing the entire evaporator fin surface to the heating plate but exposing only the lower portion of the condenser to the cooling water (No. 4) resulted in a potentially unstable situation. This is seen in the mass flow rate response curve shown in Figure 6. A small boiling excursion occurred at about 800 s but

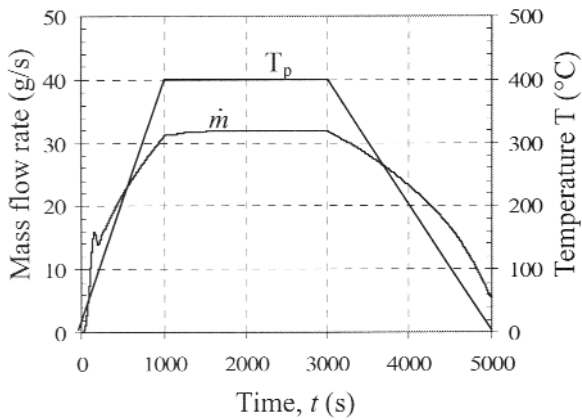


**Figure 3: Loop mass flow rate and heating plate temperature as a function of time for base case**

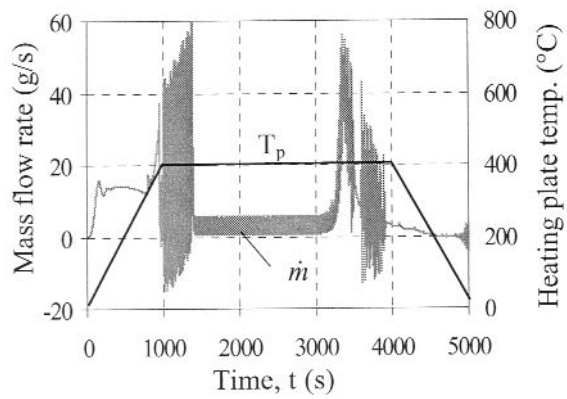


**Figure 6: Mass flow rate as a function of time response curve for No. 4 in Table 2**

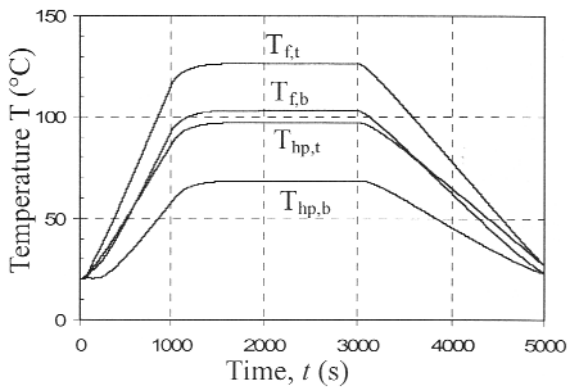


**Figure 4: Fin temperatures and loop top and bottom temperatures as a function of time for base case**

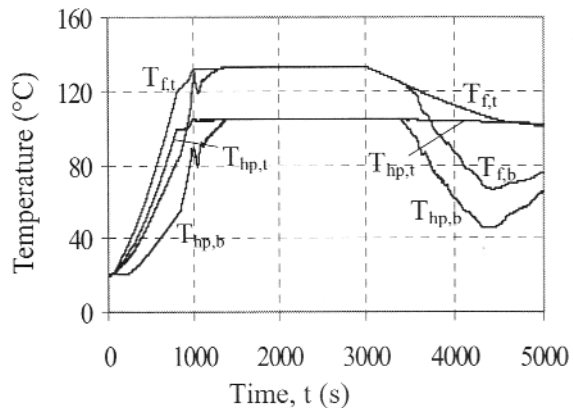


**Figure 7: Fin temperatures and loop top and bottom temperatures as a function of time for No. 4 in Table 2**

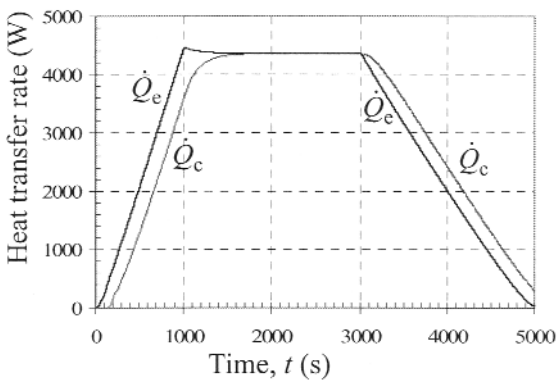


**Figure 5: Heated and cooled heat transfer rate as a function of time for the base case**

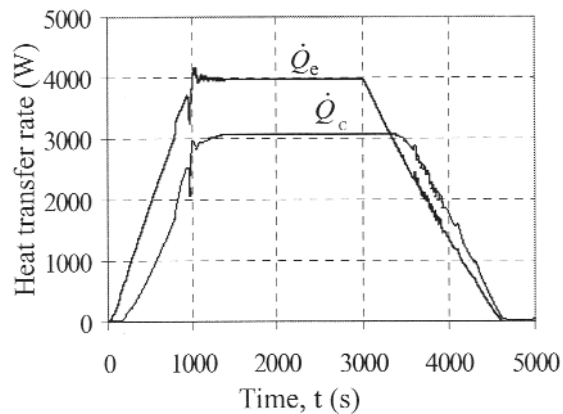


**Figure 8: Heated and cooled heat transfer rates as a function of time for No. 4 in Table 2**

soon thereafter, as the heating plate temperature increases towards its maximum of 400°C, large fluctuations in mass flow rate occur until a point is reached when the void fraction in the loop is very close to unity and relatively stable fluctuations of about 1 to 3 g/s are simulated. These oscillations (during which liquid moves into, and back from, the expansion tank) continue until just after the temperature of the heating plate starts to fall. As the heat-

ing plate temperatures fall a number of large flow rate excursions occur, and the flow rate drops off to zero.

It is thus seen that the single phase operating mode as reflected in Figure 3 (case 1) differs significantly from the two-phase operating mode shown in Figure 6 (case 4). The difference is especially dramatic when boiling starts as reflected by the first series of oscillations. It is equally dramatic when the

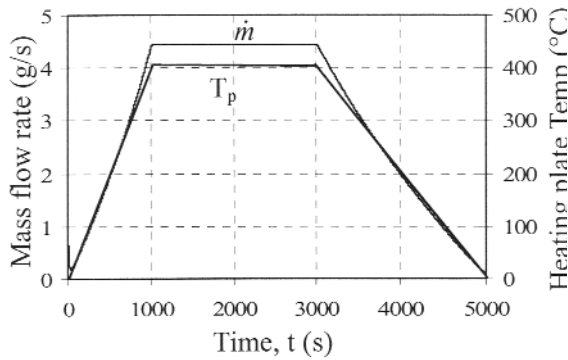


**Figure 9: Working fluid mass flow rate and heating plate temperature as a function of time for heat pipe operating mode (case 9 in Table 2)**

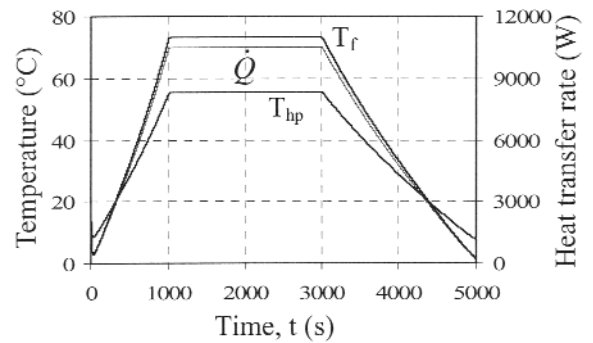


**Figure 10: Working fluid and Fin temperatures and heat transfer rate as a function of time for heat pipe operating mode (case 9 in Table 2)**

heating plate temperature starts to decrease as reflected by the second series of disturbances in Figure 6. Figures 7 and 8 are also for case 4 and give the plate and working fluid temperatures and evaporator and condenser heat transfer rates. The oscillatory behaviour when boiling starts is also seen to occur in these figures. Figures 7 and 8 can be regarded as typical of the two-phase operating mode whereas figures are similar but for the single phase operating mode.

Figures 9 and 10 reflect the response of the mass

flow rate, fin and working fluid temperature and heat transfer rates for the *heat pipe* operating mode to the given heating plate temperature profile given in figure 3. In these figure it is seen that although reasonable average values are determined no oscillatory behaviour is reflected. This is because the theoretical model uses a single control volume to simulate the working fluid and hence the dynamic behaviour of the working fluid as flows around the loop cannot be captured.

**Table 2: Sensitivity analysis**

| No. | Description  | $\dot{m}$<br>(g/s) | $\dot{Q}_{hp}$<br>(W) | $T_{f,b}$<br>(°C) | $T_{f,t}$<br>(°C) | $T_{hp,b}$<br>(°C) | $T_{hp,t}$<br>(°C) |
|-----|--|--------------------|-----------------------|-------------------|-------------------|--------------------|--------------------|
| 1   | Base case (as per figure 1 and table 1 and figures 3 to 5) | 32                 | 4400                  | 103               | 128               | 68                 | 98                 |
|     | Maximum loop static pressure varied:                       |                    |                       |                   |                   |                    |                    |
| 2   | $P_{max} = 220$ kPa  | 32                 | 4400                  | 103               | 128               | 68                 | 98                 |
|     | Loop geometry  |                    |                       |                   |                   |                    |                    |
| 3   | $L_{cw} = 0.75$ m, $L_{clw} = 0.75$ m, $L_e = 0.75$ m      | 44                 | 2000                  | 105               | 110               | 73                 | 82                 |
| 4   | $L_{cw} = 0.75$ m (figures 6, 7 and 8)                     | 5                  | 3950                  | 133               | 133               | 106                | 106                |
|     | Maximum heating plate temperature varied:                  |                    |                       |                   |                   |                    |                    |
| 5   | $T_{rv} = 200$ °C  | 22                 | 1800                  | 70                | 56                | 58                 | 38                 |
| 6   | $T_{rv} = 600$ °C  | 6                  | 7400                  | 157               | 157               | 106                | 106                |
|     | Emissivity varied:   |                    |                       |                   |                   |                    |                    |
| 7   | $\epsilon_p = \epsilon_t = 0.1$                            | 31                 | 4120                  | 122               | 98                | 94                 | 66                 |
| 8   | $\epsilon_p = \epsilon_t = 0.8$                            | 67                 | 5200                  | 136               | 123               | 101                | 85                 |
| 9   | Heat pipe operating mode (figures 9 and 10)                | 4.4                | 11 000                | 74                | 74                | 56                 | 56                 |
| 10  | $P_{max} = 70$ kPa   | 144                | 4400                  | 112               | 104               | 78                 | 85                 |

## 5. Discussion and conclusions

It is seen in the figures showing the simulation results that the theory is able to capture the transient and dynamic as well as a number of non-linear effects for the single and single and two-phase operating modes. For the heat pipe operating mode however, by virtue of the fact that all the working fluid in the loop is considered as only one control volume, the loop mass flow rate, the temperature and heat transfer rate response curves follow the heating plate temperature curve closely as well as without any suddenly-occurring oscillations. It is thus suggested that the relatively simple theoretical simulation model for the heat pipe operating mode is somewhat limited and thus needs to be improved before it can adequately capture start-up and operating transients.

In order not to unnecessarily complicate the theoretical model the values of the inside heat transfer coefficients were assumed to be constants of value as indicated in Table 1. (Also, it is unlikely that any existing heat transfer rate correlations are appropriate for this specific geometry and operating mode.) The assumed constant inside heat transfer coefficient of  $1200 \text{ W/m}^2\text{K}$  and the heat transfer rate of  $3950 \text{ W}$  are both probably too high as it is likely that the heat transfer coefficient will decrease as the void fraction tends to unity as then the flow consists essentially of only the gaseous phase with its characteristically lower heat transfer coefficient. This aspect will need to be addressed in the theoretical model of the loop so as to more accurately predict its heat transfer characteristics.

The constant values for the inside heating and cooling heat transfer coefficients for the heat pipe operating mode as reflected in Table 1 are representative of average experimental values for closed two-phase thermosyphons, i.e. for straight pipe rather than loop shaped thermosyphons. Although these values are fairly reasonable averages, they are not necessarily accurate for the different working fluid flow patterns that occur, neither are they necessarily accurate for a closed loop thermosyphon. It is thus suggested that more applicable experimentally determined heat transfer coefficients be determined taking the anticipated geometry as well as scaling factors into account.

## Nomenclature

|       |  |
|-------|--|
| $A$   | Area, $\text{m}^2$                                 |
| $C_f$ | coefficient of friction                            |
| $c_p$ | specific heat at constant pressure, $\text{J/kgK}$ |
| $c_v$ | specific heat at constant volume, $\text{J/kgK}$   |
| $c$   | specific heat, $\text{J/kgK}$                      |
| $d$   | diameter, $\text{m}$                               |
| $F$   | view factor  |
| $g$   | gravitation constant, $\text{m/s}^2$               |

|               |   |
|---------------|---|
| $h$           | heat transfer coefficient, $\text{W/m}^2\text{C}$ |
| $i$           | enthalpy, $\text{J/kg}$                           |
| $k$           | thermal conductivity, $\text{W/m}^2\text{C}$      |
| $L$           | length, length of control volume, $\text{m}$      |
| $\dot{m}$     | mass transfer rate, $\text{kg/s}$                 |
| $m$           | mass, $\text{kg}$                                 |
| $N$           | total number of control volumes                   |
| $P$           | pressure, $\text{Pa}$                             |
| $\dot{Q}$     | heat transfer rate, $\text{W}$                    |
| $r$           | radius, $\text{m}$                                |
| $R$           | thermal resistance, $^\circ\text{C}$              |
| $\text{Re}$   | Reynolds number                                   |
| $T$           | temperature, $^\circ\text{C}$                     |
| $t$           | time, $\text{s}$ or thickness, $\text{m}$         |
| $u$           | internal energy, $\text{J}$                       |
| $X$           | Martenelli parameter                              |
| $x$           | mass fraction                                     |
| $\alpha$      | void fraction                                     |
| $\theta$      | inclination to vertical                           |
| $\phi^2$      | two-phase frictional multiplier                   |
| $\rho$        | density, $\text{kg/m}^3$                          |
| $\sigma$      | Stefan-Boltzman constant                          |
| $\varepsilon$ | emissivity  |
| $\mu$         | viscosity, $\text{kg/ms}$                         |

## Subscripts

|                |                                     |
|----------------|-------------------------------------|
| $b$            | bottom                              |
| $c$            | convection, condensation            |
| $cw$           | cooling water                       |
| $e$            | environment, evaporator             |
| $\text{equiv}$ | equivalent                          |
| $f$            | friction, fin, or fluid             |
| $h$            | height                              |
| $hp$           | heat pipe                           |
| $i$            | inside                              |
| $k$            | working fluid control volume number |
| $l$            | liquid                              |
| $o$            | outside, only                       |
| $p$            | (heating) plate                     |
| $r$            | radiation                           |
| $t$            | turbulent, top, tank                |
| $v$            | vapour                              |
| $w$            | width                               |
| $x$            | cross-section                       |

## Acknowledgement

The support and assistance given by PBMR (Pty) Ltd is hereby acknowledged.

## References

- Carey, V.P., *Liquid-Vapour Phase-Change Phenomena*, Hemisphere, 1992.
- Dobson, R.T., Transient response of a closed loop thermosyphon, *R & D J.*, 1993 Vol. 9, No. 1, pp. 32-38.
- Dobson, R.T., A Novel Closed Loop Thermosyphon Heat Pipe Reactor Cavity Cooling System for a Pebble Bed



- Modular Reactor, *8<sup>th</sup> Int. Heat Pipe Symp.*, Kumamoto, 24-27 Sept. 2006, pp. 397-384.
- Greif, R., Natural circulation loops, *J. Heat Transfer*, 1988, vol. 110, pp. 1243-1258.
- Knaai, A., Zvirin, Y., Investigation of a two-phase natural circulation loop, *Proc. Int. Heat Transfer Conf., Jerusalem*, 1990, Vol. 1, pp. 395-400.
- Knaai, A., Zvirin, Y., Bifurcation phenomenon in two-phase natural circulation, *Int. J. Multiphase Flow*, 1993, Vol. 19, No. 6, pp. 1129-1151.
- Lee, S. Y. and Kim, Y. L., An analytical investigation of the role of expansion tank in semi-closed two-phase natural circulation loop, *Nucl. Eng. Des.*, 1999, Vol. 190, pp. 353-360.
- Lee, J.D., Pan, C., Non-linear analysis for a nuclear-coupled two-phase natural circulation loop, *Nucl. Eng. Des.*, 2005, vol. 235, pp. 613-626.
- Lee, Y. and Rhi, S.H., Lumped and Sectoral (Flow Pattern) Methods for Computer Simulation of Two-Phase Loop Thermosyphons, *Proc. 6<sup>th</sup> IHPS*, Chiang Mai, 2000, pp. 14-23.
- Ruppersberg, J.C. and Dobson, R.T., Flow and heat transfer in a closed loop thermosyphon Part II – Experimental evaluation, *J. Energy Southern Africa*, 2007, Vol. 18, No. 4, pp xxx-xxx.
- Vincent, C.J. and Kok, J.B.W., Investigation of the overall transient performance of the industrial two-phase closed loop thermosyphon, *Int. J. Heat Mass Transfer*, 1992, Vol. 35, No. 6, pp. 1419-1426.
- Yun G, et al. Two-phase instability analysis in natural circulation loops of China advanced research reactor, *Annals of Nuclear Energy*, 2005, Vol. 32, pp. 379-397.
- Welander, P., *J. Fluid Mech.*, 1967, Vol. 29, Part 1, pp. 17-30.
- Whalley, P.B., *Boiling Condensation and Gas-liquid Flow*, Oxford, 1987.

*Received 20 February 2007; revised 6 August 2007*